



**HAL**  
open science

# Uncertainty propagation for nonlinear vibrations: A non-intrusive approach

Alfonso Panunzio, Loic Salles, Christoph W Schwingshackl

► **To cite this version:**

Alfonso Panunzio, Loic Salles, Christoph W Schwingshackl. Uncertainty propagation for nonlinear vibrations: A non-intrusive approach. *Journal of Sound and Vibration*, 2017, 389, pp.309-325. 10.1016/j.jsv.2016.09.020 . hal-01544991

**HAL Id: hal-01544991**

**<https://hal.science/hal-01544991>**

Submitted on 22 Jun 2017

**HAL** is a multi-disciplinary open access archive for the deposit and dissemination of scientific research documents, whether they are published or not. The documents may come from teaching and research institutions in France or abroad, or from public or private research centers.

L'archive ouverte pluridisciplinaire **HAL**, est destinée au dépôt et à la diffusion de documents scientifiques de niveau recherche, publiés ou non, émanant des établissements d'enseignement et de recherche français ou étrangers, des laboratoires publics ou privés.



Distributed under a Creative Commons Attribution - NonCommercial - NoDerivatives 4.0 International License

# Uncertainty propagation for nonlinear vibrations: a non-intrusive approach

A.M. Panunzio<sup>a,b</sup>, L. Salles<sup>a</sup>, C. W. Schwingshackl<sup>a</sup>

<sup>a</sup>*Vibration University Technology Centre  
Department of Mechanical Engineering  
Imperial College London  
Exhibition Road  
London SW7 2AZ, UK*

<sup>b</sup>*Laboratoire MSSMat - UMR CNRS 8579, Ecole Centrale Paris,  
Grande Voie des Vignes  
92290 Chatenay-Malabry, France*

---

## Abstract

The propagation of uncertain input parameters in a linear dynamic analysis is reasonably well established today, but with the focus of the dynamic analysis shifting towards nonlinear systems, new approaches will be required to compute the uncertain nonlinear responses.

A combination of stochastic methods (Polynomial Chaos Expansion, PCE) with an Asymptotic Numerical Method (ANM) for the solution of the nonlinear dynamic systems will be presented to predict the propagation of random input uncertainties and assess their influence on the nonlinear vibrational behaviour of a system. The proposed method allows the computation of stochastic resonance frequencies and peak amplitudes based on multiple input uncertainties, leading to a series of uncertain nonlinear dynamic responses. One of the main challenges when using the PCE is thereby the Gibbs phenomenon, which can heavily impact the resulting stochastic nonlinear response by introducing spurious oscillations. A novel technique to avoid the Gibbs phenomenon will be presented in this paper, leading to high quality frequency response predictions.

A comparison of the proposed stochastic nonlinear analysis technique to traditional Monte Carlo simulations, demonstrated comparable accuracy at a significantly reduced computational cost, thereby validating the proposed approach.

*Keywords:* Nonlinear vibrations, Stochastic process, Polynomial Chaos Expansion, Asymptotic method, Gibbs phenomenon.

---

## 1. Introduction

Mechanical systems can experience nonlinear dynamic behaviour such as cubic stiffness, contact, friction, or impact, which can have a significant influence on the dynamic response of the system. In this case a conventional linear analysis becomes insufficient to describe the behaviour of the physical system and a nonlinear dynamic analysis is required. A large research effort has focused on the prediction of such nonlinear responses, where most techniques are based on numerical integration over time [1], providing accurate but computationally expensive results.

A more efficient technique to obtain the nonlinear dynamic response is the combination of the Harmonic Balance method (HBM) with a continuation predictor-corrector method [2] allowing the computation in the frequency domain. To further improve the computational efficiency of the approach, the iterations of the correction steps can be replaced by the Asymptotic Numerical

Method (ANM) [3, 4]. This method is based on a high order predictor to avoid the expensive correction step. The major restraint of the ANM is that the nonlinearities must be expressed in a quadratic form, somewhat restraining its wide applicability, especially for complex industrial problems where the non-linearities cannot be accurately represented by a polynomial quadratic form. However, several kinds of nonlinearities have been successfully processed with the ANM [5, 6, 7] leading to a significant reduction in the computational time.

With the emergence of reliable and accurate prediction techniques for the nonlinear response, the influence of uncertainties on the vibration behaviour has become of major interest to allow accurate predictions over a wide range of initial conditions. Uncertainty quantification (UQ) has been used to predict the effects of possible uncertainties, originating from manufacturing processes or operational conditions of a real structure, and to derive models that can take them into account. Traditional Monte Carlo simulations (MCS) [8] are often used for this purpose. They provide accurate results, but have very slow convergence rate, which limits their use for nonlinear dynamic analysis somewhat. To overcome some of the issues with the MCS, other stochastic methods have been suggested, including the Polynomial Chaos Expansion (PCE), introduced by Wiener [9] who represented a stochastic process using a series of Hermite polynomials with Gaussian random variables. The PCE has been successfully applied to model uncertainties in linear finite elements applications [10], where the uncertain Gaussian input parameters were expressed via the Karhunen-Loève Expansion and the system response was determined using the PCE. This technique has been generalized to non-Gaussian random variables [11, 12] using orthogonal polynomial basis adapted to any probability distribution function. In further generalisations, the PCE has been extended to rational function series [13], partitioned random space [14] and sparse chaos expansions [15], adding additional features and enabling its use for the presented nonlinear dynamic analysis with uncertainties.

The PCE has been used, in combination with the HBM, to analyse the dynamic linear response of a rotor with Gaussian uncertainties [16], saving significant computational time when compared to MCS without the loss of accuracy. For this linear case the frequency was considered to be independent of the uncertain variables which is unsuitable for a nonlinear dynamic response analysis. The latter can be characterized by returning points (and so multi-solutions) which makes the frequency non-deterministic. To overcome this issue, Didier and Sinou [17] used an intrusive PCE in combination with the HBM and a predictor-corrector method, leading to an accurate stochastic response of a nonlinear system. This approach has been successfully applied to complex mechanical problems [18], but unfortunately the intrusive nature requires a rewrite of the equations of the problem which in turn necessitates modifications to the deterministic numerical solver for each new computation. The intrusive approach also requires the definition of a stochastic phase condition which differs for each type of nonlinearity and which is usually quite difficult to find.

A large number of PCE coefficients are often required to achieve convergence of the first and second statistical moments (mean and standard deviation) to the MCS solution [19], reducing somewhat the computational advantages of PCE. To improve the efficiency of the PCE, a combination with Aitken's method has been proposed [20] leading to improved the convergence of the system.

A further problem arising from the use of the PCE is the presence of spurious oscillations in the stochastic response in case of strong discontinuities. This so called Gibbs phenomenon can strongly affect the results and introduce large differences to the reference solution (eg. MCS) [17, 21]. This is of particular relevance for nonlinear dynamic problems, where the presence of returning points in the response can lead to significant oscillations, making an accurate and reliable prediction quite challenging.

In this paper an efficient approach to compute the stochastic nonlinear dynamic response of a system will be presented, combining the PCE with the HBM and the ANM to allow an

accurate and fast computation. The introduced method can be applied as intrusive or non-intrusive approach, the latter giving it a much wider applicability for industrial application since it eliminates the need for modifications to existing deterministic solvers. The proposed technique also avoids the Gibbs oscillations, enabling an accurate and fast computation of the stochastic nonlinear dynamic response, which is further improved by the use of the the Smolyak quadrature [22] for multivariate random spaces. The resulting frequency response functions are validated against Monte Carlo Simulations (MCS).

## 2. Deterministic nonlinear problem

The chosen approach to solve the deterministic nonlinear problem is a combination of the Harmonic Balance method (HBM, [4]) with the Asymptotic Numerical Method (ANM) that allows a fast and accurate solution of the nonlinear equations. The ANM is based on an Taylor expansion of the solution [3] and its combination with HBM was first introduced by Moussi [5]. A short introduction to the HBM+ANM approach will be provided for completeness, but for a detailed discussion the reader may consult above references.

ANM is a continuation method (path-following) based on the expression of the solution in a Taylor series. The initial solution (first point) is calculated using a traditional iterative process (e.g. Newton's method) after which the solution path is followed by approximating the solution with a Taylor series. When enough terms are being used in the Taylor series, the error on the computed solution is very small, eliminating the need of the time consuming correction step of traditional path following techniques.

One of the formulations of a nonlinear dynamic system characterised by  $D$  DOFs is:

$$\mathbf{M}\ddot{\mathbf{x}}(t) + \mathbf{C}\dot{\mathbf{x}}(t) + \mathbf{K}\mathbf{x}(t) = \mathbf{F}(t) + \mathbf{F}_{nl}(t, \mathbf{x}(t), \dot{\mathbf{x}}(t)) \quad (1)$$

where  $\mathbf{M}$ ,  $\mathbf{C}$  and  $\mathbf{K}$  are respectively the mass, damping (including gyroscopic effects if needed) and stiffness matrices,  $\mathbf{x}(t)$  is the vector of the displacements (for  $n$  DOFs),  $\mathbf{F}_{nl}(t, \mathbf{x}(t), \dot{\mathbf{x}}(t))$  represents the vector of nonlinear effects in the system and  $\mathbf{F}(t)$  is the vector of the external forces.

In order to apply the ANM for the calculation of the nonlinear responses, the equations of motion (Eq. (1)) must be represented in a polynomial quadratic form to allow the use of simple algebra in the solution process. This enables a simple computation of the Taylor series coefficients, which is essential for the effectiveness of the approach. This requirement of representing the nonlinearities in a quadratic form is the main drawback of the ANM, but fortunately expressions for many common nonlinearities can be found in the literature: contact [5, 6, 7], friction [6, 7], vibro-impact [6], cubic [23]. Using these expressions, the system of equations can be written in the following form:

$$m(\dot{\mathbf{S}}) = c + l(\mathbf{S}) + q(\mathbf{S}, \mathbf{S}) \quad (2)$$

where  $c$  is a constant,  $m$  and  $l$  are linear applications and  $q$  is a quadratic (bilinear) map. All the maps go from  $\mathbb{R}^{Q+1}$  to  $\mathbb{R}^Q$ , where  $Q$  is the number of equations of the system.  $\mathbf{S}$  is a vector containing all the unknowns.

For the harmonic balance method the unknown vector  $\mathbf{S}$  is expressed as Fourier series truncated at an order  $H$  selected via a convergence study. Then the time variable  $t$  is removed by projecting the equations of motion onto the basis:

$$\mathcal{F}_H = \{1, \cos(\omega t), \sin(\omega t), \cos(2\omega t), \sin(2\omega t), \dots, \cos(H\omega t), \sin(H\omega t)\} \quad (3)$$

where  $\omega$  is the excitation frequency.

After defining the state vector  $\mathbf{U}$ , containing all the Fourier coefficients of all the DOFs and the excitation frequency, the final equation of motion becomes:

$$\mathbf{R}(\mathbf{U}) = \mathbf{L}_0 + \mathbf{L}(\mathbf{U}) + \mathbf{Q}(\mathbf{U}, \mathbf{U}) = \mathbf{0} \quad (4)$$

where  $\mathbf{L}_0$ ,  $\mathbf{L}(\mathbf{U})$  and  $\mathbf{Q}(\mathbf{U}, \mathbf{U})$  are respectively a constant, linear and quadratic map going from  $\mathbb{R}^{N+1}$  to  $\mathbb{R}^N$ , where  $N$  is the total number of unknown Fourier coefficients. Once the equation of motion has been converted to this form, the ANM can be included in the solution process of the HBM to solve the nonlinear dynamic problem. If the equation of motion does not contain a forcing function, than a phase condition has to be added to close the problem [24].

The first step of the ANM is to find the initial solution of the nonlinear system (Eq. (4)) via a traditional corrector method (e.g. Newton's method). After calculating the first solution, the ANM allows to track the evolution of the system behaviour directly as the excitation frequency  $\omega$  changes. In order to obtain the next solution step (i.e. following the path), the unknown state vector  $\mathbf{U}$  is expanded to a finite Taylor series, starting from the first solution,  $\mathbf{U}_0$ , which has been found before:

$$\mathbf{U}(a) = \mathbf{U}_0 + a\mathbf{U}_1(a) + a^2\mathbf{U}_2(a) + \dots + a^z\mathbf{U}_z(a) \quad (5)$$

where  $a$  is the step length that has to be determined and  $\mathbf{U}_1, \mathbf{U}_2, \dots, \mathbf{U}_t$  are the derivatives, whose the order is indicated by the subscript, of  $\mathbf{U}$ .

Since  $\mathbf{R}(\mathbf{U})$  is a quadratic operator the calculation of the derivatives  $\mathbf{U}_i$  (with  $i = 1, \dots, z$ ) can be easily achieved by solving a set of linear systems that all have the same tangent matrix  $\mathbf{K}$  [3], i.e. the Jacobian matrix:

$$\mathbf{K}_T \mathbf{e}_j = \mathbf{L}(\mathbf{e}_j) + \mathbf{Q}(\mathbf{U}_0, \mathbf{e}_j) + \mathbf{Q}(\mathbf{e}_j, \mathbf{U}_0) \quad (6)$$

where  $\mathbf{e}_j$  is the canonical base vector (same dimension than  $\mathbf{U}_0$ ).

The path parameter  $a$  is defined as an arc-length measure, i.e. it is identified as the orthogonal projection of the state vector increment  $\mathbf{U}(a) - \mathbf{U}_0$  on the tangent vector  $\mathbf{U}_1$  (see Fig. 1). Within a region of low curvature (flat path in Fig. 1), the parameter  $a$  can be relatively large since the amplitude does not vary much, allowing a fast computation of the response curve, while in regions with high curvature (see Fig. 1) smaller step sizes must be used. A simple criterion to adapt the arc-length [3] is to ensure that the difference between two consecutive order solutions stays within a tolerance ( $\epsilon$ ):

$$\frac{\|a^z \mathbf{U}_z\|}{\|a\mathbf{U}_1 + \dots + a^z \mathbf{U}_z\|} \approx \frac{\|a^z \mathbf{U}_z\|}{\|a\mathbf{U}_1\|} \leq \epsilon \Rightarrow a \approx \left( \epsilon \frac{\|\mathbf{U}_1\|}{\|\mathbf{U}_z\|} \right)^{\frac{1}{z-1}} \quad (7)$$

The truncation order  $z$  is a compromise. It depends on the problem (shape of the solution). In practice, if the chosen truncation order is too low, the path parameter  $a$  in Eq. (7) will be small and, therefore, the number of iterations to obtain the whole solution will increase. Otherwise, if  $z$  is too large, the number of derivatives  $\mathbf{U}_i$  to compute increases. The order is usually between 10 and 20 [3].

Once the current solution  $\mathbf{U}(a)$  has been computed it is then used as the departure point to continue the iterative solution process.

The ANM allows all the nonlinear dynamic calculations associated with traditional methods, such as stability studies of the solutions [23], and bifurcation points detection [25] making it an interesting alternative to standard nonlinear solutions. It eliminates the need for the correction steps that are required for the standard path following techniques (prediction-correction methods), leading to significantly shorter computational times. The only limitation is the need to express the nonlinearities in a quadratic form, which may limit its applicability to certain problems.

The HBM+ANM approach is of particular interest for this uncertainty propagation investigation, since the improved computational time allows a much faster statistical analysis of the nonlinear problems. The step-wise continuous function of the solution curve can also be used to improve computational time, unlike the discrete points of the solution curve that is the results of the classical predictor-corrector method.

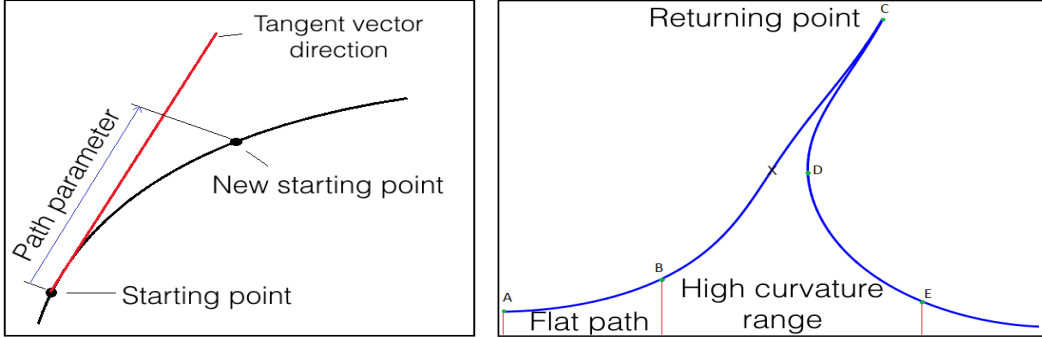


Figure 1: Asymptotic Numerical path-following Method: Path-parameter in ANM (left) and Path-following technique (right).

### 3. Polynomial Chaos Expansion

When the input parameters of a system of equations are defined by random distributions, than the propagation of the uncertainties in the model can be studied with stochastic methods. Once such approach is the Polynomial Chaos Expansion [9, 10, 11, 12, 26] which will shortly be presented in this section for completeness. It significantly reduced the computational effort of a stochastic analysis when compared to traditional MCS, making it an interesting choice for the calculation of a stochastic nonlinear dynamic response.

The general idea behind the PCE is to express a generic stochastic output (e.g. amplitude of displacements, frequency,...) as a sum of polynomial functions of random input variables. When considering a random multivariate variable  $\xi$  (random vector collecting all the random inputs), defined in a random space  $\Omega$  of dimension  $d$ , with a cumulative distribution function  $F_{\xi}(\xi)$  and finite moments, the generalised polynomial chaos expansion of a stochastic function  $Y(\xi)$  is:

$$Y(\xi) = \sum_{k=0}^P \beta_k \Psi_k(\xi) \quad (8)$$

where  $\beta_k$  are the deterministic coefficients of the basis that have to be calculated,  $\Psi_k(\xi)$  is the polynomial chaos basis functions, and  $P$  is the order of the polynomial. If the cumulative density function (CDF) exists so that  $dF_{\xi}(\xi) = p(\xi)d\xi$ , with  $p(\xi)$  being the probability function (PDF) of the random variable  $\xi$ , than the polynomial chaos basis functions are the orthogonal polynomial functions satisfying:

$$\langle \Psi_n(\xi), \Psi_m(\xi) \rangle = \int_{\Omega} \Psi_n(\xi) \Psi_m(\xi) p(\xi) d\xi = \gamma_n \delta_{mn} \quad \text{with } m, n = 0, \dots, P \quad (9)$$

where  $\gamma_n$  are constants and  $\delta_{mn}$  is the Kronecker delta. Eq. 9 establishes a correspondence between the distribution of the random input variable  $\xi$  and the orthogonal polynomials of its PCE basis. The polynomial basis for the most common PDFs can be found in literature [12, 26].

The inner product of Eq. (9) with respect to the PDF will be indicated by the symbol  $\langle \bullet, \bullet \rangle$  to simplify the expressions.

For a random space of dimension,  $d$ , and a maximum polynomial expansion degree,  $p$ , (also called chaos degree), the number of terms,  $P$ , in Eq. (8) is determined:

$$P + 1 = \frac{(d + p)!}{d!p!} \quad (10)$$

The last remaining parameters required for Eq. 8 are the coefficients,  $\beta_k$ , which can either be calculated via an intrusive or non-intrusive approach. This calculation will be discussed in more detail in the next section.

#### 4. Linking of ANM and PCE

Different approaches can be used to calculate the PCE coefficients ( $\beta_k$ ). The equations can either be projected onto the orthogonal space of the polynomials [26] or a collocation method can be used. The first approach, often referred to as Galerkin method, can be intrusive or non-intrusive depending the way the inner products are calculated whereas the latter method is a non-intrusive projection. To demonstrate the capabilities of both approaches, they will be adapted in this work for use with the ANM to allow a fast computation of stochastic nonlinear responses.

##### 4.1. Intrusive stochastic Galerkin method

For the intrusive approach the PCE coefficients are directly calculated by solving a set of equations obtained from the Galerkin projection (inner product). The unknown of the deterministic system in Eq. (4), i.e. the state vector  $\mathbf{U}$ , is thereby replaced with the PCE coefficients. In other words, in the Galerkin based approach, the deterministic PCE coefficients are calculated by solving the system of equations derived by forcing the residual to be orthogonal to the approximation space [26]. For the intrusive approach the equations of the deterministic problem have to be rewritten as a nonlinear algebraic problem, leading to a system of coupled equations with the same properties as the original system. This technique has been used successfully in combination with the HBM and a predictor-corrector method by Didier *et al.* [17] to compute stochastic nonlinear responses, and it will now be expanded to the Asymptotic Numerical Method to allow for a faster computation.

To express the random response  $\mathbf{U}(\boldsymbol{\xi})$  with the PCE formulation of Eq. (8)), Eq. (4) has to be rewritten as:

$$\hat{\mathbf{R}}(\boldsymbol{\beta}) = \hat{\mathbf{L}}_0 + \hat{\mathbf{L}}(\boldsymbol{\beta}) + \hat{\mathbf{Q}}(\boldsymbol{\beta}, \boldsymbol{\beta}) = \mathbf{0} \quad (11)$$

where  $\boldsymbol{\beta}$  is the vector containing all the PCE coefficients which represents the unknown of the system. The objective is to obtain the stochastic maps,  $\hat{\mathbf{L}}_0$ ,  $\hat{\mathbf{L}}(\boldsymbol{\beta})$ , and  $\hat{\mathbf{Q}}(\boldsymbol{\beta}, \boldsymbol{\beta})$ , going from  $\mathbb{R}^{(N+1) \times (P+1)}$  to  $\mathbb{R}^{N \times (P+1)}$ , so that  $\boldsymbol{\beta}$  can be computed. For this purpose the definition of orthogonality in Eq. (9) is exploited.

The constant application becomes:

$$\begin{aligned} \hat{\mathbf{L}}_0 &= [\hat{\mathbf{L}}_{00}, \dots, \hat{\mathbf{L}}_{0k}, \dots, \hat{\mathbf{L}}_{0P}]^T \\ \hat{\mathbf{L}}_{0k} &= \langle \mathbf{L}_0, \Psi_k(\boldsymbol{\xi}) \rangle \quad \text{with } k = 0, \dots, P \end{aligned} \quad (12)$$

The linear application  $\mathbf{L}(\mathbf{U}(\boldsymbol{\xi}))$  can be written in the form  $\mathbf{A}\mathbf{U}(\boldsymbol{\xi})$ , where  $\mathbf{A}$  is the deterministic linear application matrix. Applying the Galerkin projection to the linear application matrix  $\mathbf{A}$

leads to the stochastic linear application matrix  $\hat{\mathbf{A}}$ :

$$\hat{\mathbf{A}} = \begin{bmatrix} \mathbf{A}_{00} & \cdots & \mathbf{A}_{0P} \\ \vdots & \mathbf{A}_{ij} & \vdots \\ \mathbf{A}_{P0} & \cdots & \mathbf{A}_{PP} \end{bmatrix} \quad \text{with } \mathbf{A}_{ij} = \langle \Psi_i(\boldsymbol{\xi})\mathbf{A}(\boldsymbol{\xi}), \Psi_j(\boldsymbol{\xi}) \rangle; \quad i, j = 0, \dots, P \quad (13)$$

leading to  $\hat{\mathbf{L}}(\boldsymbol{\beta}) = \hat{\mathbf{A}}\boldsymbol{\beta}$ .

The quadratic application  $\mathbf{Q}(\mathbf{U}(\boldsymbol{\xi}), \mathbf{U}(\boldsymbol{\xi}))_n$  from Eq. (4) can be expressed as:

$$\begin{aligned} \mathbf{Q}(\mathbf{U}(\boldsymbol{\xi}), \mathbf{U}(\boldsymbol{\xi})) &= [q_1, \dots, q_n, \dots, q_N]^T \\ q_n &= \mathbf{U}(\boldsymbol{\xi})^T \mathbf{B}_n(\boldsymbol{\xi}) \mathbf{U}(\boldsymbol{\xi}) \quad \text{with } n = 1, \dots, N \end{aligned} \quad (14)$$

where  $N$  is the number of equations of the deterministic system and  $\mathbf{B}_n(\boldsymbol{\xi})$  are the bilinear application matrices. The stochastic quadratic operator  $\hat{\mathbf{Q}}(\boldsymbol{\beta}, \boldsymbol{\beta})$  can then be obtained via a projection of the  $\mathbf{B}_n(\boldsymbol{\xi})$  matrices with the Galerkin method:

$$\hat{\mathbf{Q}}(\boldsymbol{\beta}, \boldsymbol{\beta}) = \boldsymbol{\beta}^T \hat{\mathbf{B}}_p \boldsymbol{\beta}, \quad \text{with } p = 1, \dots, N(P+1) \quad (15)$$

Finally the bilinear stochastic application matrix  $\hat{\mathbf{B}}_p$  is calculated:

$$\hat{\mathbf{B}}_p = \begin{bmatrix} \mathbf{B}_{n00} & \cdots & \mathbf{B}_{n0P} \\ \vdots & \mathbf{B}_{nij} & \vdots \\ \mathbf{B}_{nP0} & \cdots & \mathbf{B}_{nPP} \end{bmatrix} \quad \text{with } \mathbf{B}_{nij} = \langle \Psi_i(\boldsymbol{\xi})\Psi_j(\boldsymbol{\xi})\mathbf{B}_n(\boldsymbol{\xi}), \Psi_k(\boldsymbol{\xi}) \rangle; \quad (16)$$

$$i, j = 0, \dots, P; \quad k = \lfloor \frac{p-1}{N} \rfloor; \quad n = p - kN$$

where  $\lfloor \bullet \rfloor$  denotes the *floor* function.

The number of variables in the state vector  $\mathbf{U}$  is  $N+1$  (where  $N$  is the number of equations, i.e. total number of Fourier coefficients) for the deterministic asymptotic method. After the stochastic Galerkin projection, the number of equations will become  $N(P+1)$  and the number of variables in state vector (in this case the state vector contains the stochastic modes) will be  $(N+1)(P+1)$ . In order to solve the stochastic problem,  $P$  other equations have to be added to the system in Eq. (11) since to apply the ANM, the difference between the number of unknowns and the number of equations must be equal to one. Didier [17] proposes the use of the following stochastic phase condition for this purpose:

$$\sum_{h=1}^H (\boldsymbol{\beta}_{0_{hcos}} \cdot \boldsymbol{\beta}_{k_{hsin}} - \boldsymbol{\beta}_{0_{hsin}} \cdot \boldsymbol{\beta}_{k_{hcos}}) = 0 \quad \text{with } k = 1, \dots, P \quad (17)$$

where the symbol  $\cdot$  denotes the dot product and the subscript  $k_{hcos}$  ( $k_{hsin}$ ) indicates the sub-vector containing all the  $k$ -degree polynomial chaos coefficients related to the cosine (sine) harmonics.

Also a continuation method has been used in [17] instead of the ANM, the interpretation of Eq (17) stays the same, where the phase difference between the mean response and the stochastic solution is set to zero. This means that the phase of the stochastic solution computed with the PCE+ANM does not depend on the random variables (it is deterministic) while the amplitude of the response is uncertain.

A summary of the PCE+ANM approach with an intrusive Galerien projection can be seen in Fig. 2 to further clarify the working of the procedure. The main advantage of the approach is that only a single system of equations (also much larger) has to be solved and the PCE coefficients can be directly computed. Unfortunately the equations have to be rewritten in order to be solved, which makes its use with many existing solvers (existing finite element code for example) quite complicated, somewhat limiting it's use to research applications. Finally the stochastic phase

condition in Eq. (17) is only valid if the phase is deterministic and for the case where the phase depends on the uncertainties, a different condition must be used, requiring an adaptation of the intrusive approach for each new problem.

To overcome these limitations, a non-intrusive approach has been developed for the PCE+AMN technique, which leads to a much wider applicability.

#### 4.2. Non-intrusive collocation method

In deterministic numerical analysis, non-intrusive collocation methods (NICM) are a family of approaches that require the residual of the governing equations to be zero at discrete nodes (collocation points) in the computational domain. The NICM solves a finite number of deterministic problems extracted from the stochastic problem by replacing the random variables with deterministic values allowing the use of existing codes to compute the response. The resulting deterministic solutions of the collocation points is then being used to determine the information about the full stochastic response.

The selection of the collocation points is thereby critical to ensure an accurate extraction of the stochastic response. For deterministic sampling methods, the nodal set is often defined by a Gaussian quadrature rule [26] where the  $M$  collocation points in a one-dimensional random space correspond to the zeros of the  $M^{th}$  degree polynomial of the basis. The aim of this method is to conduct a discrete projection by using the definition of orthogonality from Eq. (9):

$$\beta_k = \frac{\langle y(\boldsymbol{\xi}), \Psi_k(\boldsymbol{\xi}) \rangle}{\gamma_k} \quad (18)$$

which means that the stochastic modes can be computed by solving a series of integrals with the expression  $y(\boldsymbol{\xi})$  being unknown at this stage. Fortunately the integrals can be approximated with the cubature formulas. Given a set of  $M$  collocation points and their associated normalized weights (according to the PDF),  $M$  deterministic solutions  $y(\boldsymbol{\xi})$  can be calculated, leading to the final equation for  $\beta_k$ :

$$\beta_k = \frac{1}{\gamma_k} \sum_{i=1}^M y(\boldsymbol{\xi}_i) \Psi_k(\boldsymbol{\xi}_i) w_i \quad (19)$$

that is based on a set of deterministic solutions that can be readily computed. The steps of the non-intrusive method are summarized in Fig. 2.

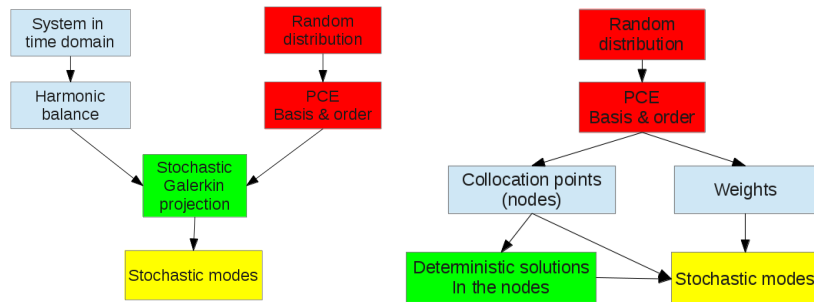


Figure 2: Calculation of the PCE coefficients: Intrusive stochastic Galerkin(left) and Non-intrusive collocation (right).

The Gaussian quadrature can be expanded to multivariate random spaces ( $d > 1$ ) with the help of the Gaussian cubature [12, 26]. The easiest approach to calculate the stochastic modes for the entire multivariate space is thereby the use of a tensor product. Unfortunately the number of collocation points thereby increases exponentially with the dimension  $d$ , potentially requiring

the computation of a large number of solutions and significantly reducing the advantage of the PCE over the MCS. One way to reduce the total number of nodes while maintaining the accuracy offered by the Gaussian cubature is to use the Smolyak sparse grids cubature [22]. The size of the Smolyak grid depends on the dimension of the random space. For most cases there is no explicit formula available to know how many points are needed for a given random space dimension, but the number of collocation points for the Smolyak sparse grid cubature is always smaller than for the tensor product technique (see Fig. 3), leading to a significantly reduced computational effort. To further highlight the difference between the two collocation point approaches, Fig. 4 shows the tensor and Smolyak grids for a bi-dimensional (Normal-Uniform) random space (with chaos degree=3 and Smolyak grid level=2) where it can be seen that, when a tensor product cubature is used, 32 more runs are needed to compute the integral.

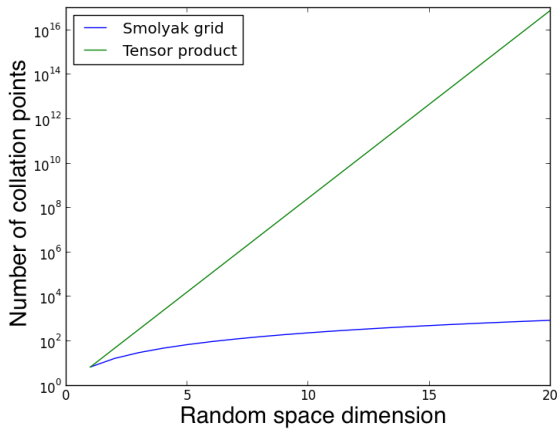


Figure 3: Smolyak vs. tensor product, (with chaos degree=3 and Smolyak grid level=2).

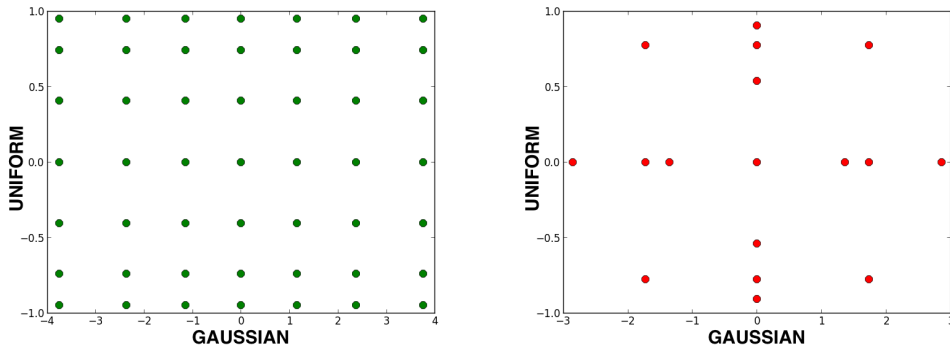


Figure 4: Tensor product (left) and Smolyak grids(2D random space, with PCE degree=3).

## 5. A solution for the Gibbs phenomenon

The PCE approximates the relationship between random input and output space with the help of polynomial functions. Sometimes in a mechanical system, especially if it is nonlinear, the response can be strongly discontinuous [26] which prevents the output to be expressed as a polynomial function, leading to spurious oscillations in the proximity of the discontinuity. This behaviour is often referred to as the Gibbs phenomenon and it can for instance appear when a

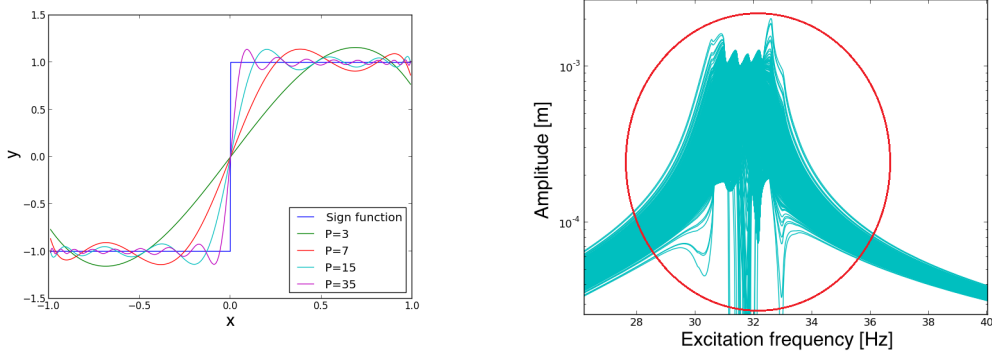


Figure 5: Examples of Gibbs phenomena: polynomial approximation of the *sign* function for different polynomial orders  $P$  (left) and Gibbs phenomenon in FRF (Case A of Table 1).

sign function is being approximated by a polynomial (see Fig. 5). An increase in the polynomial order leads to a decrease of the the oscillation (the polynomial approximation converges on the target) but the oscillations still affect the results, as long as the polynomial degree is not extremely high [19] where they become negligible at the cost of a large computational effort.

In a nonlinear frequency response function (FRF) these spurious oscillations can become very large, especially near the amplitude peaks and the turning points (i.e. the points where the frequency response experiences a strong change in direction) as shown in Fig. 5 for a slightly stiffening nonlinearity. The Gibbs phenomenon in the response clearly leads to wrong values in the stochastic FRFs, making an accurate evaluation of the results difficult, and an approach is therefore needed to ensure a correct computation.

The use of the Padé-Legendre expansion has been proposed [13] to avoid the Gibbs phenomenon in a physical system with strong discontinuities. The general idea of this technique is to express the stochastic response using a rational function of random uniform variables which successfully allows avoiding the Gibbs phenomenon, but unfortunately also leads to artificial peaks which affect the stochastic response. These peaks occur when the denominator of the rational function tends towards zero and their effect will be shown in Section 7). The Padé-Legendre expansion is only valid for uniform random variables which limits it's use practical use further and a different technique is therefore required to compute the full and accurate stochastic response of nonlinear dynamic systems without the effects of the Gibbs phenomenon .

In this section a new technique to avoid the Gibbs phenomenon for a nonlinear vibration problems is presented, based on the general idea of limiting the discontinuities in the surface response for non-intrusive stochastic methods.

The response frequency of a linear vibration problem can be considered deterministic (not dependent on the random variables) and at the collocation point (non-intrusive method), only one response can be found since the random variables are unique. For a nonlinear problem more than one solution may exist due to the presence of returning points, for a given set of frequency and random variables. Thereby the position of the returning points (and the amplitude peaks) will depend on the random variables leading to a stochastic frequency and the response. Since these stochastic parameters can not be selected for the continuation method, a different, deterministic, parameter is required to ensure a smooth response curve.

One possible deterministic parameter for the calculation of the PCE coefficients is a fixed arc-length  $a$  in Eq. (5) for each step of the ANM in all collocation points (see Fig. 6). Unfortunately this approach alone does not solve the problem, since in some regions, especially in the vicinity of the amplitudes peaks, the Gibbs phenomenon can still strongly impact the response. This

happens when the amplitudes for some collocation points are still increasing at a given arc-length while, due to the nonlinearity, the amplitudes of other collocation points are already decreasing. For instance, if, for a given arc-length, the solution has already passed a resonance peak for some collocation points (and not for all), a strong discontinuity can appear in the stochastic response. In addition, if for a given arc-length, the solutions of some collocation points have already passed a returning point, their frequencies are decreasing, while they may still increase for the other collocation points, leading to further strong discontinuities and the appearance of the Gibbs phenomenon. A fixed arc length on its own is therefore not suitable to make the nonlinear problem deterministic.

In order to avoid this phenomenon a new approach has been developed. It permits to solve stochastic nonlinear problems with very strong nonlinearities and avoid Gibbs phenomenon. It is based on the previous idea of a fixed arc length, but one replaces it with an "arc length ratio".

At first all the significant variation points in the FRF, such as the start and end of FRF, the amplitudes maxima and minima, and the returning points (if present), are detected (see Fig. 7). In a next step each section between two variation points is divided into smaller segments by the "arc length ratio" ( $\frac{a}{A}$ ), where  $A$  is the total arc length between two variation points for each FRF. In this way the deterministic parameter is not the arc-length measure but the ratio, ensuring that maxima and turning points are reached at the same time in the calculation of the PCE coefficients (see Fig. 6), eliminating the discontinuities in the system, and therefore the appearance of the Gibbs phenomenon.

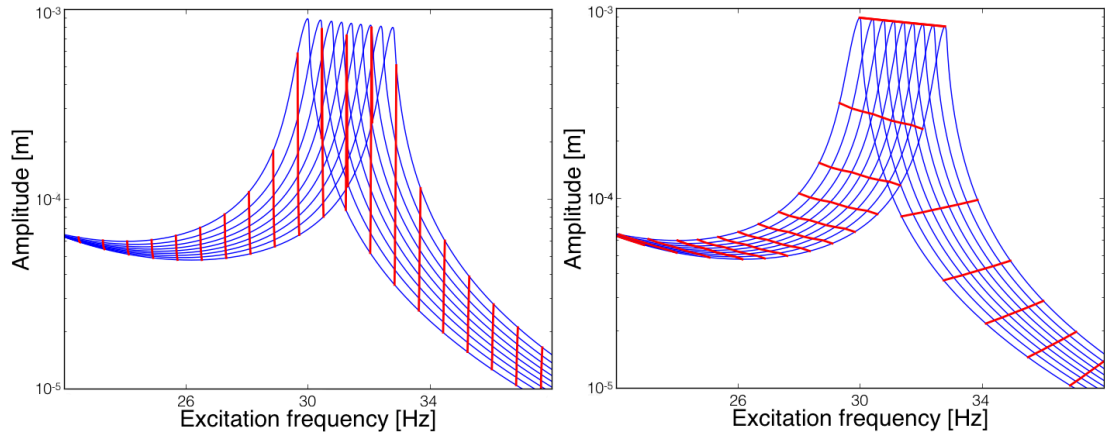


Figure 6: Frequency response based on NICM with different arc length technique: NICM with deterministic arc length (left) and NICM with deterministic arc length ratio (right).

To better explain the introduce process (see flow chart in Fig. 8), the application of the technique to the FRF from Fig. 7 will be discussed in detail. Once the responses in the collocations points have been computed, the variation points (amplitudes peaks and returning points) are detected. For the deterministic FRFs in the  $M$  collocation points in Fig. 7 the amplitude extrema are the points (b),(d),and (e), and the returning points are (b) and (c). These points are used to define the arc-length ratio which is taken as deterministic parameter for the PCE coefficients calculation. In a first step the total arc length ( $A_i(\xi_i)$  with  $i = 1, \dots, M$ ) between points (a) and (b) is calculated for each collocation point solution, and the arc-length ratio steps,  $h_i = \frac{a_i(\xi_i)}{A_i(\xi_i)}$ , are calculated ( $h_i \in [0, 1]$ ). At each step the PCE coefficients are calculated using the non-intrusive projection that is expressed as:

$$\begin{pmatrix} \langle \Psi_0(\xi), \Psi_0(\xi) \rangle \beta_0 \\ \vdots \\ \langle \Psi_P(\xi), \Psi_P(\xi) \rangle \beta_P \end{pmatrix} = \begin{bmatrix} \Psi_0(\xi_1) & \cdots & \Psi_0(\xi_M) \\ \vdots & \vdots & \vdots \\ \Psi_P(\xi_1) & \cdots & \Psi_P(\xi_M) \end{bmatrix} \begin{pmatrix} y(\xi_1, \frac{a_1}{A_1})w_1 \\ \vdots \\ y(\xi_M, \frac{a_M}{A_M})w_M \end{pmatrix} \quad (20)$$

where  $a_1, \dots, a_M$  are the current arc length and  $A_1, \dots, A_M$  are the total arc lengths between the two variation points (a) and (b). The solutions are taken at the same arc length ratio ( $\frac{a_i}{A_i} = \frac{a_j}{A_j}$ , with  $i, j = 1, \dots, M$ ) ensuring that no discontinuities appear in the segment, leading to the computation of the stochastic response with no Gibbs phenomenon.

By repeating the process between the points (b) and (c), and so on, the global stochastic response can be obtained. The strong discontinuities are avoided since the technique ensures that the critical points are reached at the same time.

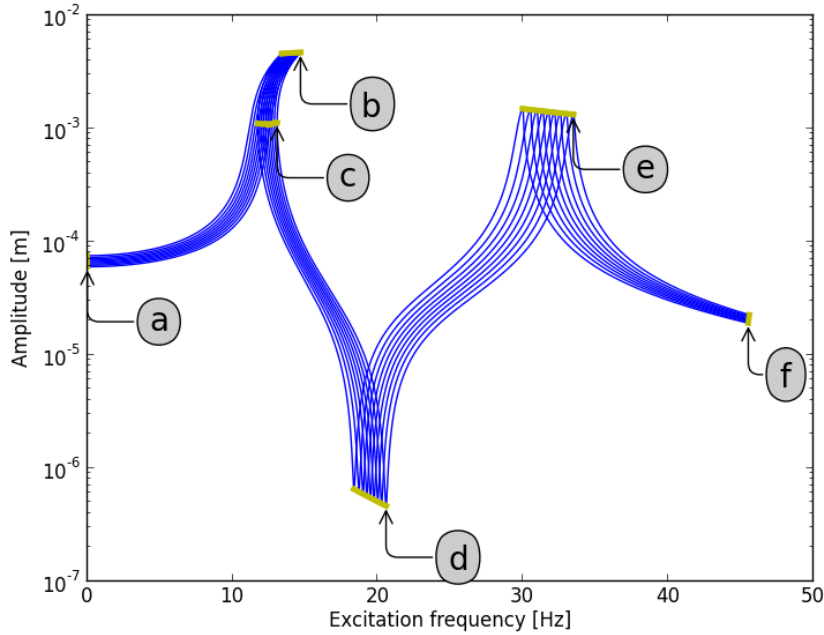


Figure 7: Response in the collocation points, case A in Table 1, 1st harmonic 1st DOF displacement.

## 6. Numerical studies

A simple 2DOFs model, shown in Fig. 9, is used to validate the proposed method for calculating the stochastic response of a nonlinear system. Note that the model is the same than the one used in [17]. A cubic nonlinearity ( $f_{nl}$ ) is placed between the ground and the first DOF and a periodic force ( $f_1 = f \cos(\omega t)$ ) is applied on the first DOF. This simple system is being used to highlight the effect of stochastic input parameters on the nonlinear dynamic response, and allow a reliable comparison of the new technique to deal with the Gibbs phenomenon to more traditional approaches.

Several cases summarized in Table 1, with a different number of uncertain linear and nonlinear parameters (i.e. random space dimension), are considered to gain a better understanding of their significance on the nonlinear dynamic response. Note that the cases A and B are equal respectively to the cases 1 and 2ter in [17].

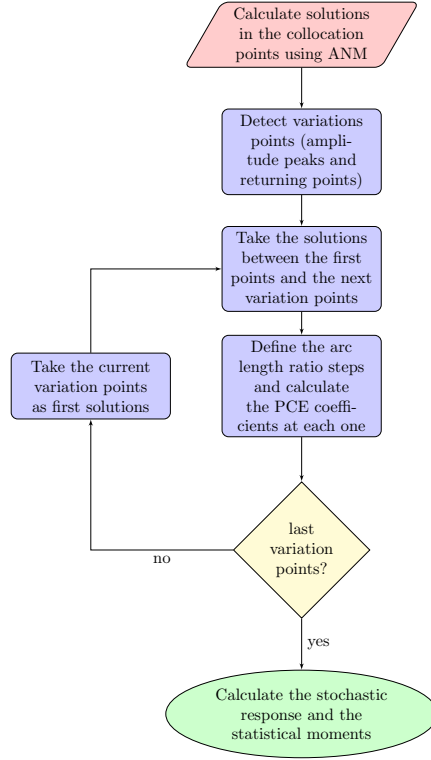


Figure 8: PCE + ANM with deterministic arc length ratio.

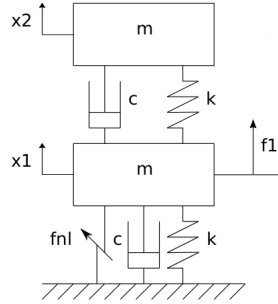


Figure 9: 2 DOFs model, from [17].

Case	$k$ [ $Nm^{-1}$ ]	$c$ [ $Nsm^{-1}$ ]	$m$ [ $kg$ ]	$k_{nl}$ [ $Nm^{-3}$ ]	$f$ [ $N$ ]	$\xi$ PDF	PCE basis
A	$1.5^4(1 + 0.025\xi)$	1	1	$5^8$	1	$\mathcal{N}(0, 1)$	Hermite
B	$1.5^4$	1	1	$5^{10}(1 + 0.1\xi)$	1	$\mathcal{N}(0, 1)$	Hermite
C	$1.5^4(1 + 0.025\xi_1)$	1	1	$5^{10}(1 + 0.1\xi_2)$	1	$\mathcal{N}(0, 1)$ $\mathcal{U}(-1, 1)$	Hermite Legendre
D	$1.5^4(1 + 0.025\xi_1)$	1	$1(1+0.075\xi_2)$	$5^{10}(1 + 0.1\xi_3)$	1	$\mathcal{N}(0, 1)$ $\mathcal{U}(-1, 1)$ $\mathcal{U}(-1, 1)$	Hermite Legendre Legendre

Table 1: Numerical studies.

In case A the uncertainty is on the linear stiffness,  $k$ , while the small nonlinear coefficient,

$k_{nl}$  is kept constant. In case B, the nonlinear coefficient is uncertain and its mean value is 100 times larger than in case A. Case C applies the uncertainty to both the linear and the nonlinear stiffness. The final case D adds an additional uncertainty to the mass leading to a three dimensional stochastic space.

In Table 1 the notations  $\mathcal{N}(0, 1 =$  and  $\mathcal{U}(-1, 1)$  indicate respectively a centred Normal (Gaussian) with unitary standard deviation and an Uniform distributions between -1 and 1.

## 7. Results

The two non-intrusive techniques, based on the deterministic arc length and the deterministic arc length ratio, from Section 5 have been used to calculate the PCE coefficients and compute the stochastic response for the different cases from Table 1. The results are compared to MCS responses in Fig. 10 to 13. The average response (mean value), standard deviation and 95% and 5% percentiles are indicated on the figures. In order to compare the PCE with the MCS, the solutions generated through PCE are obtained with the same random seed than MCS (same samples).

In the computation of the nonlinear response only the first 3 harmonics are considered in the HBM, since it could be shown that they lead to converged results. The polynomial chaos order of each case is set to 3 which was the minimum required to match the reference Monte Carlo solution with 1000 iterations (Fig. 10 to 13). The number of collocation points which depend on the chosen polynomial degree is set to 9 for cases A and B (unidimensional random spaces). For multivariate random spaces the Smolyak grid quadrature technique is used to reduce the number of collocation points: in cases C and D the number of collocation points is respectively 17 and 31

When the arc-length measure is taken as the deterministic parameter, Fig. 10 to 13 show that the Gibbs phenomenon significantly affects the stochastic response, leading to an over and under-estimation of the amplitudes around the resonance peaks, when compared to the MCS results. Instead the use of the newly developed technique from Section 5 based on the arc length ratio leads to a much better agreement between the PCE and the MCS results (see Fig. 10 to 13) with no spurious oscillations in the response.

The response of case A in Fig. 10 with a uncertain linear stiffness mainly shows a shift in resonance frequency due to the uncertainty. Due to the nonlinear behaviour of the system (the coupling between the linear and the nonlinear operators), the amplitude peaks and the returning points are also affected by the linear random variable. When the PCE coefficients are calculated using the arc length as deterministic parameter, big discontinuities appear around the peaks leading to a strong Gibbs phenomenon. It is interesting to observe, that even there is no returning point at the second resonance peak (weakly nonlinear), the Gibbs phenomenon has a big impact on this mode. This can be linked to the higher sensitivity of the second mode to the uncertain linear stiffness, which leads to larger discontinuities for a given fixed arc length. The new proposed technique with the arc length ratio is able to cope with this situation (Fig. 10), leading to very clean results.

In the case B the order of magnitude of nonlinear coefficient  $k_{nl}$  is increased hundred times to study the effect of the uncertainties on a strongly nonlinear system. The nonlinear coefficient is considered to be uncertain. It can be observed in Fig. 11 that the increase of the nonlinear cubic stiffness leads to a very strong hardening behaviour of the mechanical system. Since the uncertainty is introduced on the nonlinear coefficient, it has a big impact on the peaks and the returning points of the FRF, but it does not affect the rest of the FRF, where the nonlinearity is only mildly activated. Using the PCE with a deterministic arc length (see Fig. 7), the Gibbs phenomenon only has a minor impact on the first resonance peak where the uncertain nonlinear

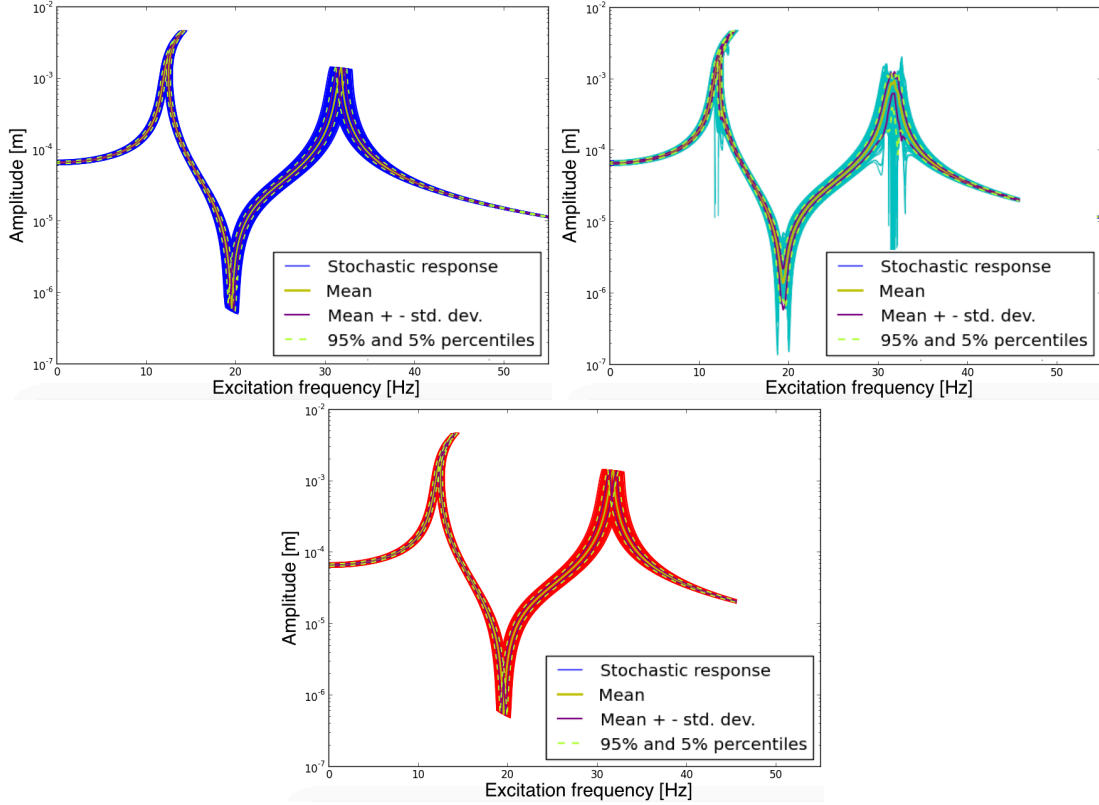


Figure 10: Case A, 1st harmonic displacement, 1st DOF: MCS (top left), Deterministic arc length PCE (top right), Deterministic arc length ratio NICM (bottom).

coefficient does not deeply change the solutions in the region far from the resonance peaks so that the total arc length is about the same for each collocation point. In contrast a very strong oscillations can be observed for the second mode, where the extreme overhang leads to strong discontinuities. The stochastic position of the returning points (due to the nonlinear effect) and the influence of the random variable on them are well described with the proposed new method (Fig. 11), leading to very similar responses when compared to the MCS.

For the case C a bi-dimensional random space is tested, with an uncertain linear and nonlinear stiffness. It was observed before, that the linear stiffness affects the entire FRF, whereas the nonlinear stiffness only has an impact on the resonance peaks. The combination of these two effect is shown in Fig. 12. Once more the entire FRF has become uncertain due to the linear influence, also the location of the resonance peaks is slightly less spread out than for case B. This is due to the use of an uniform (and so bounded) distribution for the nonlinear coefficient in case C which differs from the Gaussian distribution of the case B.

For the arc length approach the Gibbs phenomenon appears strongly at the second resonance peak because of the strong return due to the nonlinearity (Fig. 12), but it also shows up at the antiresonance due to the uncertainty of the linear component. A comparison to the MCS results shows that the mean response of the arc-length PCE is not too different but the standard deviation and the 5% and 95% percentiles are very different due to the strong impact of the Gibbs oscillations. Using the method proposed in this paper, the stochastic solution is identical to the MCS results (Fig. 12) and accurate stochastic values can be computed. Thanks to the use of the Smolyak grid cubature the number of collocation points could be reduced from 49 for a tensor product cubature to 17 without a loss of accuracy.

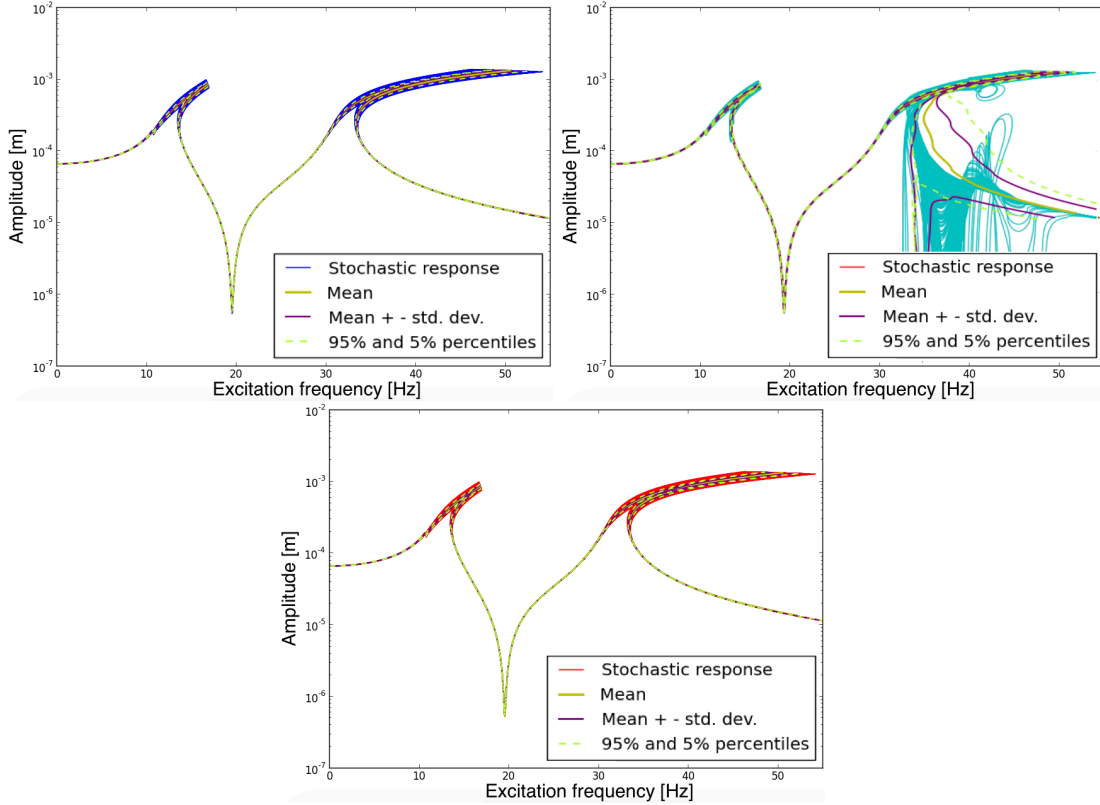


Figure 11: Case B, 1st harmonic displacement, 1st DOF: MCS (top left), Deterministic arc length PCE (top right), Deterministic arc length ratio NICM (bottom).

For the case D a third uncertainty is added to the mass. As a result the envelope of the stochastic response in Fig. 13 is now wider than for case C, but otherwise the shape of the resulting FRFs is not strongly impacted. Due to the wider spread of the FRFs, the impact of the Gibbs phenomenon (Fig. 13) is even stronger than for case C, if the deterministic parameter is the arc-length, since the increase in the dimension of the random space, adds more discontinuities to the stochastic response. Even for multidimensional space the proposed new technique with the arc-length ratio allows to calculate a stochastic PCE response that matches the MCS (Fig. 13) results. Due to the larger random space the Smolyak cubature is even more efficient, reducing the required collocation points from 343 for the tensor product to 31.

For the case B,C and D, an internal resonance, due to the strong nonlinearity, can be found on the FRF around  $\omega = 10.5Hz$ . The proposed method is able to capture this small peak in the stochastic response, as shown for the case D in Fig. 7 making it applicable for quite complicated nonlinear dynamic response computations. Fig. 14 shows as the stochastic response of the third harmonic of the displacement of the first DOF is well obtained with the PCE.

As mentioned in the previous section, an alternative approach to eliminate the Gibbs phenomenon is the use of the Padé-Legendre expansion (rational polynomial function). For completeness its results for case A are shown in Fig. 15. It can be seen, that the Gibbs phenomenon that was present around the resonance and antiresonance region in Fig. 10 can be avoided, but some other spurious peaks appear in the stochastic response envelope. This is caused either by the non-existence of a polynomial for the denominator whose zeros are close to the discontinuity locations, or the denominator may have zeros where there are no discontinuities. When the later occurs, a huge peak is generated in the stochastic response that has no physical meaning. A

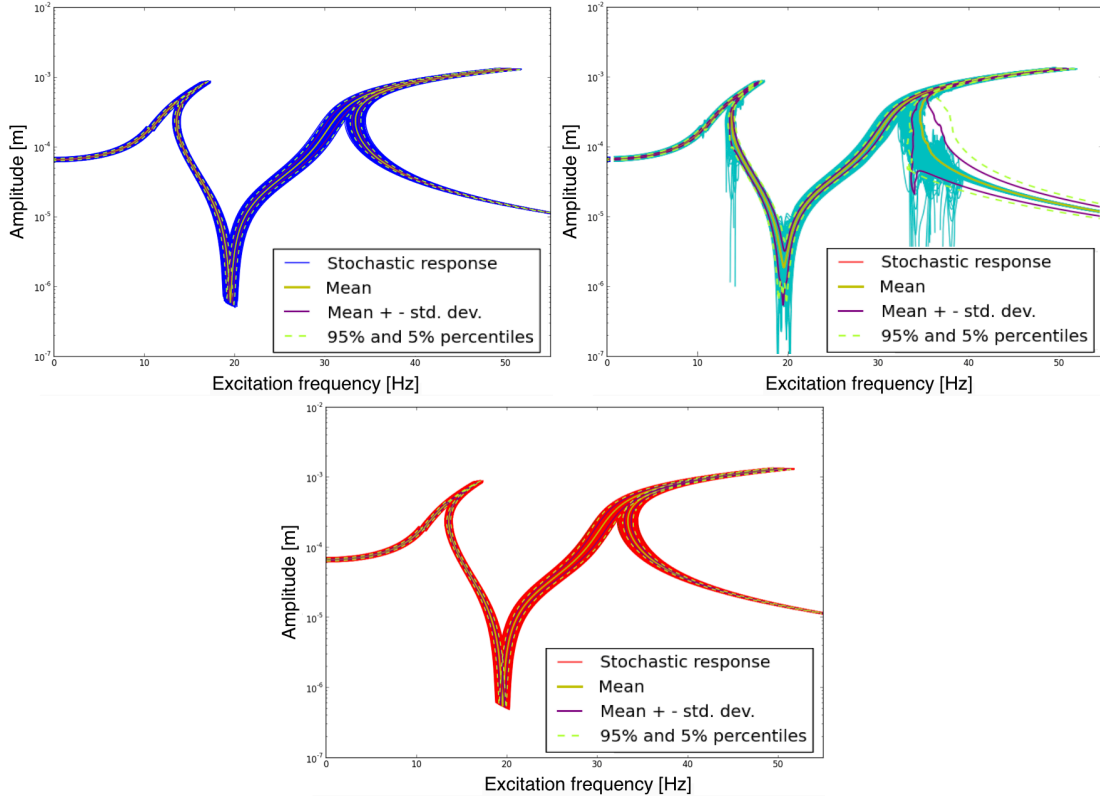


Figure 12: Case C, 1st harmonic displacement, 1st DOF: MCS (top left), Deterministic arc length PCE (top right), Deterministic arc length ratio NICM (bottom).

proper combination of the orders of the numerator and denominator at each step, which can be found with an iterative process [13], allows to overcome this problem, but at large computational cost, which makes it rather unsuitable for stochastic nonlinear dynamic response calculations.

In [17], the uncertainties are propagated into the model using an intrusive technique and the Gibbs phenomenon is avoided. The issue with the intrusive approach is that the equations of the problem need to be rewritten and the existing deterministic solver codes cannot be used without modifications. Moreover, in [17] a stochastic phase condition (Eq. (17)) needs to be added to close the problem. This condition requires that the phase does not depend on the uncertainties (it is deterministic).

To quantify the accuracy and computational efficiency of the proposed approach, case D has been analysed further. An error concerning the standard deviation of the amplitude peaks has been evaluated as:

$$err = \frac{|\hat{f}_{1000} - \hat{f}_n|}{\hat{f}_{1000}} + \frac{|\hat{A}_{1000} - \hat{A}_n|}{\hat{A}_{1000}} \quad (21)$$

where  $\hat{A}$  and  $\hat{f}$  are respectively the standard deviation of the displacement amplitude and the frequency at a resonance peak, while the subscripts indicates the number of samples in the MCS. The results of a convergence study of the MCS can be seen in Fig. 16 where the error shown is the maximal between all the resonance peaks. At least 750 iterations are required in the MCS to obtain stable results whereas in comparison the PCE with a deterministic arc length ratio obtains the same results (less than 1% error) with only 31 iterations due the Smolyak cubature. This leads to a 25 time reduction in computational time and makes the approach well suited for nonlinear dynamic analysis. Fig. 17 shows the agreement between MCS and PCE (mean and

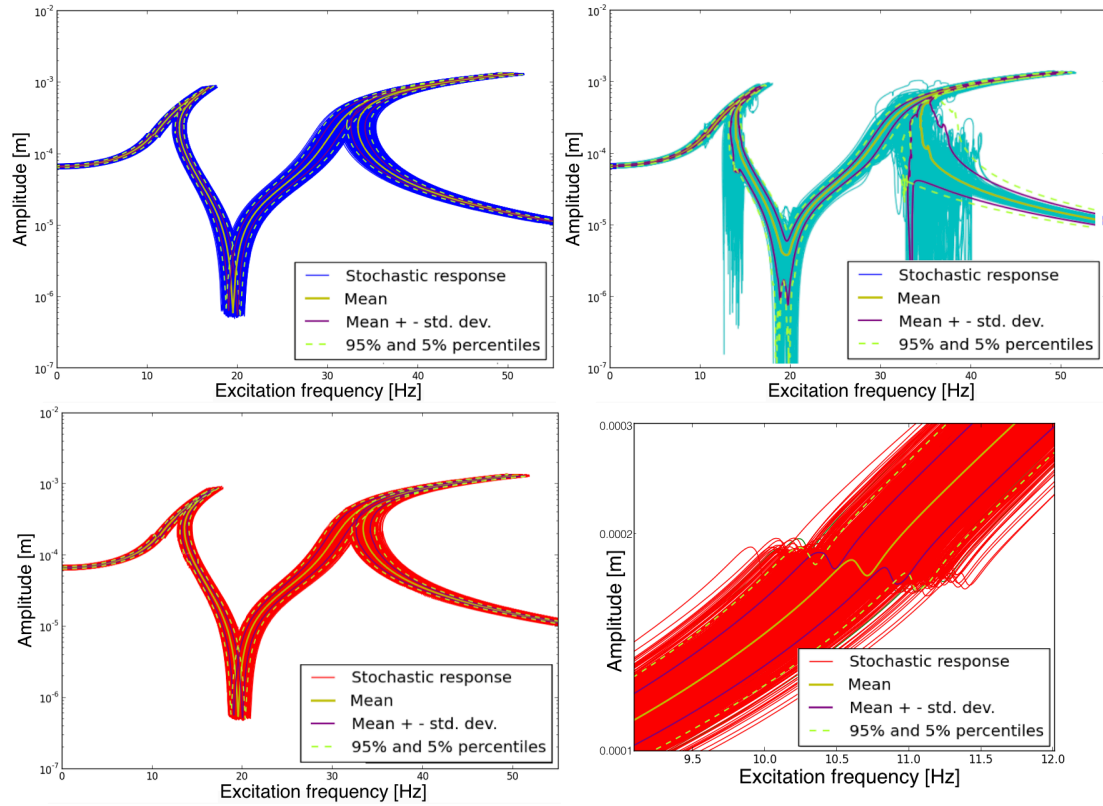


Figure 13: Case D, 1st harmonic displacement, 1st DOF: MCS (top left), Deterministic arc length PCE (top right), Deterministic arc length ratio NICM (bottom left), zoom on the internal resonance peak (bottom right).

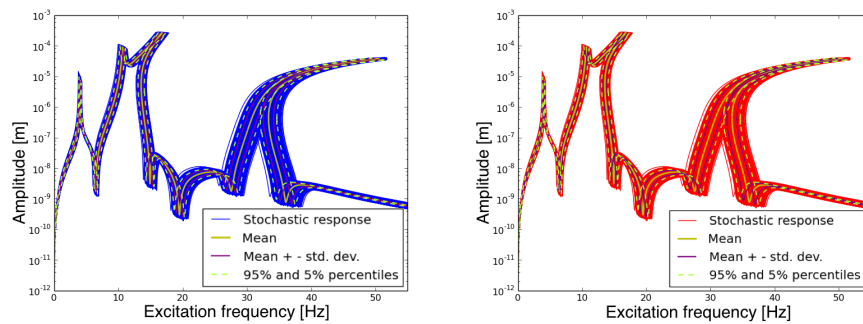


Figure 14: Case D, 3rd harmonic displacement, 1st DOF: MCS (left), Deterministic arc length ratio NICM (right).

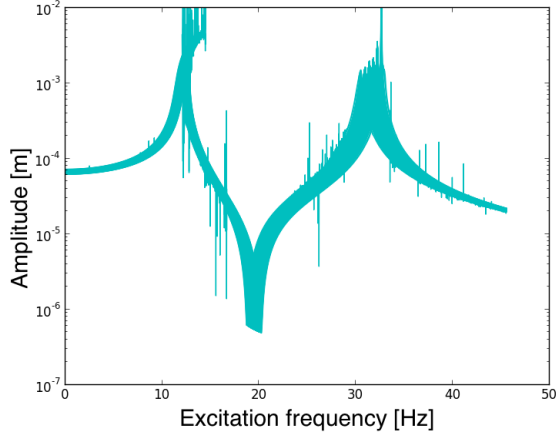


Figure 15: Padé-Legendre expansion, case A, 1st harmonic displacement, 1st DOF.

mean  $\pm$  standard deviation) over the entire frequency range, where no visible difference in the response can be observed.

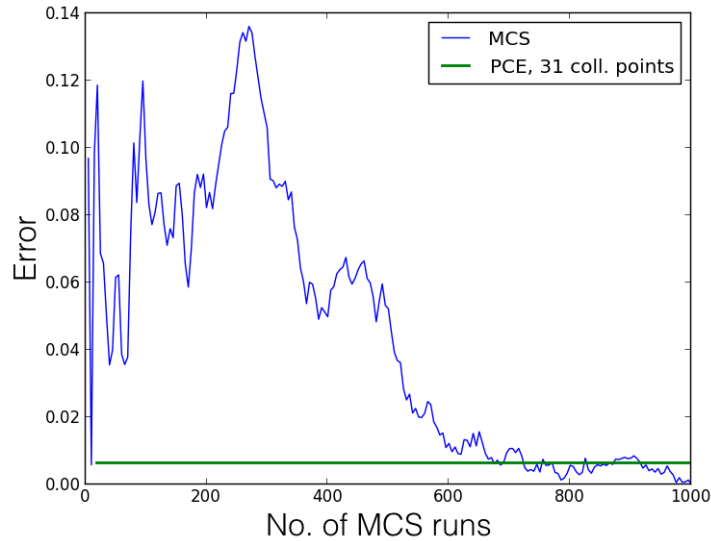


Figure 16: MCS convergence and PCE error for case D.

In this section the proposed method has been validated by using a small two DOFs system. The same method has been successfully applied in some more complicated analysis as the stochastic calculation of the nonlinear normal modes of a FEM model of a rotor blade with contact non-linearity [28] and FRFs in nonlinear rotor-dynamics with uncertainties [29]. In [28], the method described in this paper has been successfully applied using 13 harmonics in the simulations. More complicated cases, with hundreds of harmonics, have not yet been performed with this method. Note that in some test cases analyzed in [29], the uncertainties affect the symmetry of the system and the appearance of secondary resonance peaks in the response for some collocation points. This is an issue, if one wants to apply the technique proposed in this paper, because the appearance of these secondary peaks makes the peaks detection matching harder (differently of the easy peaks detection shown in Fig. 7). Indeed, as explained in Section 5, firstly the peaks are detected for each collocation point response, then their are paired in order to compute the PCE

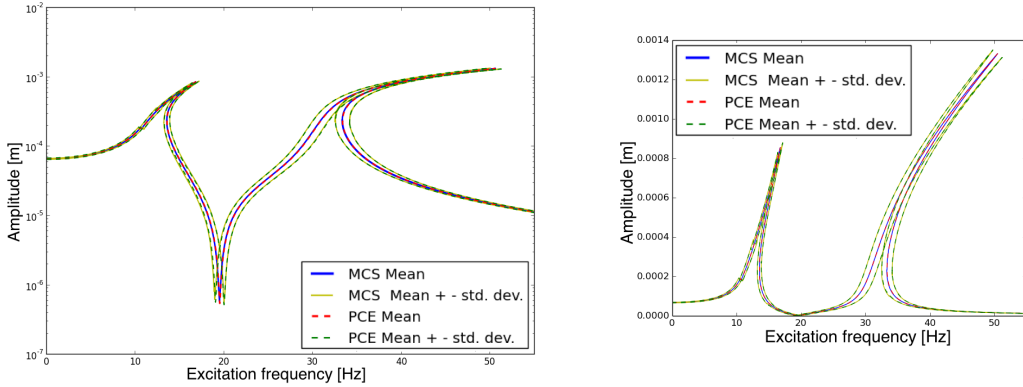


Figure 17: Mean and standard deviation responses for MCS and PCE, case D: Amplitude in logarithmic scale (left), Amplitude in linear scale (right).

coefficients as in Eq. (20). Therefore, for the application of this method, the peaks detection and pairing is an essential step. When some secondary peaks appear only in some collocation point responses, the pairing of the peaks is not straightforward as in Fig. 7. Two possible solutions can be adopted to outcome this issue. One possibility is discarding the secondary peaks and directly using Eq. (20) to calculate the PCE coefficients. This leads to a good stochastic representation around the main resonance peaks, but a possible discrepancy near the secondary peaks. Another strategy, successfully adopted in [29], is partitioning the random space in sub-spaces so that the peaks detection and pairing is simpler: the domain of the integral of Eq. (18) is broken into sub-spaces such that, in each sub-space, the responses of the collocation points present the same resonance behaviour concerning the secondary peaks.

## Conclusion

This paper studies the stochastic nonlinear dynamic response of an excited system. The use of Monte Carlo methods for nonlinear dynamic systems with uncertainties can be too expensive in terms of computation time and data storage, and therefore a stochastic approach, based on polynomial chaos, is proposed.

The introduced technique is a non-intrusive PCE combining Harmonic Balance and the Asymptotic Numerical method to solve a nonlinear dynamic problem. To overcome the major drawback of the appearance of the Gibbs phenomenon in the stochastic nonlinear response, a novel technique has been introduced that allows the fast and accurate computation of uncertain nonlinear FRFs. It proposes the use of a deterministic arc length ratio to avoid the strong discontinuities in the nonlinear response, leading to stochastic FRFs that are in excellent agreement with the Monte Carlo Sampling results, even for multivariate random spaces. The use of the Smolyak cubature rule in combination with the non-intrusive PCE leads to a significant reduction in computational time when compared to Monte Carlo Sampling method.

## References

- [1] M. Géradin, D. J. Rixen, Mechanical vibrations: theory and application to structural dynamics, John Wiley & Sons, 2014.
- [2] E. Sarrouy, J.-J. Sinou, Non-Linear Periodic and Quasi-Periodic Vibrations in Mechanical Systems - On the use of the Harmonic Balance Methods, in: F. Ebrahimi (Ed.), Advances

- in *Vibration Analysis Research*, InTech, Rijeka, Croatia, 2011, Ch. 21, pp. 419–434, ISBN: 978-953-307-209-8. [doi:10.5772/15638](https://doi.org/10.5772/15638).
- [3] B. Cochelin, A path-following technique via an asymptotic-numerical method, *Computers & Structures* 53 (5) (1994) 1181 – 1192. [doi:10.1016/0045-7949\(94\)90165-1](https://doi.org/10.1016/0045-7949(94)90165-1).
  - [4] B. Cochelin, C. Vergez, A high order purely frequency-based harmonic balance formulation for continuation of periodic solutions, *Journal of Sound and Vibration* 324 (12) (2009) 243 – 262. [doi:10.1016/j.jsv.2009.01.054](https://doi.org/10.1016/j.jsv.2009.01.054).
  - [5] E. H. Moussi, S. Bellizzi, B. Cochelin, I. Nistor, Nonlinear normal modes of a two degree of freedom oscillator with a bilateral elastic stop, in: XVIII th symposium Vibrations Chocs et Bruit & ASTELAB, EDF R&D Clamart, France, 2012.
  - [6] S. Karkar, B. Cochelin, C. Vergez, A high-order, purely frequency based harmonic balance formulation for continuation of periodic solutions: The case of non-polynomial nonlinearities, *Journal of Sound and Vibration* 332 (4) (2013) 968 – 977. [doi:10.1016/j.jsv.2012.09.033](https://doi.org/10.1016/j.jsv.2012.09.033).
  - [7] H. Zahrouni, W. Aggoune, J. Brunelot, M. Potier-Ferry, Asymptotic Numerical Method for strong nonlinearities, *Revue Européenne des Éléments Finis* 13 (1-2) (2004) 97–118. [doi:10.3166/reef.13.97-118](https://doi.org/10.3166/reef.13.97-118).
  - [8] N. Metropolis, S. Ulam, The Monte Carlo Method, *Journal of the American statistical association* 44 (247) (1949) 335–341. [doi:10.1080/01621459.1949.10483310](https://doi.org/10.1080/01621459.1949.10483310).
  - [9] N. Wiener, The Homogeneous Chaos, *American Journal of Mathematics* 60 (4) (1938) 897–936. [doi:10.2307/2371268](https://doi.org/10.2307/2371268).
  - [10] R. G. Ghanem, P. D. Spanos, *Stochastic finite elements: a spectral approach*, Courier Dover Publications, Dover, New York, 2003.
  - [11] C. Soize, R. Ghanem, Physical Systems with Random Uncertainties: Chaos Representations with Arbitrary Probability Measure, *SIAM Journal on Scientific Computing* 26 (2) (2004) 395–410. [doi:10.1137/S1064827503424505](https://doi.org/10.1137/S1064827503424505).
  - [12] D. Xiu, G. E. Karniadakis, The Wiener-Askey Polynomial Chaos for Stochastic Differential Equations, *SIAM J. Sci. Comput.* 24 (2) (2002) 619–644. [doi:10.1137/S1064827501387826](https://doi.org/10.1137/S1064827501387826).
  - [13] T. Chantrasmi, A. Doostan, G. Iaccarino, Padé-Legendre approximants for uncertainty analysis with discontinuous response surfaces, *Journal of Computational Physics* 228 (19) (2009) 7159 – 7180. [doi:10.1016/j.jcp.2009.06.024](https://doi.org/10.1016/j.jcp.2009.06.024).
  - [14] X. Wan, G. E. Karniadakis, An Adaptive Multi-element Generalized Polynomial Chaos Method for Stochastic Differential Equations, *J. Comput. Phys.* 209 (2) (2005) 617–642. [doi:10.1016/j.jcp.2005.03.023](https://doi.org/10.1016/j.jcp.2005.03.023).
  - [15] G. Blatman, B. Sudret, Adaptive sparse polynomial chaos expansion based on least angle regression, *J. Comput. Phys.* 230 (6) (2011) 2345–2367. [doi:10.1016/j.jcp.2010.12.021](https://doi.org/10.1016/j.jcp.2010.12.021).
  - [16] J. Didier, J.-J. Sinou, B. Faverjon, Study of the non-linear dynamic response of a rotor system with faults and uncertainties, *Journal of Sound and Vibration* 331 (2012) 671–703. [doi:10.1016/j.jsv.2011.09.001](https://doi.org/10.1016/j.jsv.2011.09.001).
  - [17] J. Didier, J.-J. Sinou, B. Faverjon, Nonlinear vibrations of a mechanical system with non-regular nonlinearities and uncertainties, *Communications in Nonlinear Science and Numerical Simulation* 18 (11) (2013) 3250 – 3270. [doi:10.1016/j.cnsns.2013.03.005](https://doi.org/10.1016/j.cnsns.2013.03.005).

- [18] J.-J. Sinou, J. Didier, B. Faverjon, Stochastic non-linear response of a flexible rotor with local non-linearities, *International Journal of Non-Linear Mechanics* 74 (2015) 92–99. doi:[10.1016/j.ijnonlinmec.2015.03.012](https://doi.org/10.1016/j.ijnonlinmec.2015.03.012).
- [19] E. Jacquelin, S. Adhikari, J.-J. Sinou, M. I. Friswell, Polynomial chaos expansion and steady-state response of a class of random dynamical systems, *Journal of Engineering Mechanics* 141 (4) (2015) 04014145. doi:[10.1061/\(ASCE\)EM.1943-7889.0000856](https://doi.org/10.1061/(ASCE)EM.1943-7889.0000856).
- [20] E. Jacquelin, S. Adhikari, J.-J. Sinou, M. I. Friswell, Polynomial chaos expansion in structural dynamics: Accelerating the convergence of the first two statistical moment sequences, *Journal of Sound and Vibration* 356 (356) (2015) pp. 144–154. doi:[10.1016/j.jsv.2015.06.039](https://doi.org/10.1016/j.jsv.2015.06.039).
- [21] J.-J. Sinou, E. Jacquelin, Influence of Polynomial Chaos expansion order on an uncertain asymmetric rotor system response, *Mechanical Systems and Signal Processing* 5051 (0) (2015) 718 – 731. doi:[10.1016/j.ymsp.2014.05.046](https://doi.org/10.1016/j.ymsp.2014.05.046).
- [22] S. Smolyak, Quadrature and interpolation formulas for tensor products of certain classes of functions, *Soviet Mathematics, Doklady* 4 (1963) 240–243.
- [23] A. Lazarus, O. Thomas, A harmonic-based method for computing the stability of periodic solutions of dynamical systems, *Comptes Rendus Mécanique* 338 (9) (2010) 510 – 517. doi:[10.1016/j.crme.2010.07.020](https://doi.org/10.1016/j.crme.2010.07.020).
- [24] A. H. Nayfeh, B. Balachandran, *Applied nonlinear dynamics: analytical, computational and experimental methods*, John Wiley & Sons, 2008.
- [25] B. Cochelin, M. Medale, Power series analysis as a major breakthrough to improve the efficiency of Asymptotic Numerical Method in the vicinity of bifurcations, *Journal of Computational Physics* 236 (0) (2013) 594 – 607. doi:[10.1016/j.jcp.2012.11.016](https://doi.org/10.1016/j.jcp.2012.11.016).
- [26] O. P. Le Maître, O. M. Knio, *Spectral Methods for Uncertainty Quantification : with applications to computational fluid dynamics*, Series: Scientific computation, Springer, Dordrecht, Heidelberg, London, 2010.
- [27] V. Kaarnioja, [Smolyak Quadrature](#), Master’s thesis, University of Helsinki (Helsingin yliopisto), Department of Mathematics and Statistics (2013). URL <https://helda.helsinki.fi/handle/10138/40159>
- [28] A. M. Panunzio, L. Salles, C. Schwingshackl, M. Gola, Asymptotic Numerical Method and Polynomial Chaos Expansion for the study of Stochastic Non-linear Normal Modes, in: *ASME Turbo Expo*, American Society of Mechanical Engineers, Montreal, 2015. doi:[10.1115/GT2015-43560](https://doi.org/10.1115/GT2015-43560).
- [29] E. Peradotto, A. M. Panunzio, L. Salles, C. Schwingshackl, Stochastic methods for Nonlinear Rotordynamics with Uncertainties, in: *ASME Turbo Expo*, American Society of Mechanical Engineers, Montreal, 2015. doi:[10.1115/GT2015-43534](https://doi.org/10.1115/GT2015-43534).